

Surface Organometallic Chemistry of Titanium on Silica–Alumina and Catalytic Hydrogenolysis of Waxes at Low Temperature

Cherif Larabi, Nicolas Merle, Sébastien Norsic, Mostafa Taoufik, Anne Baudouin, Christine Lucas, Jean Thivolle-Cazat, Aimery de Mallmann,* and Jean-Marie Basset*

Université Lyon 1, Institut de Chimie de Lyon, Lyon, France, Université Lyon 1, CPE Lyon, CNRS, UMR 5265 C2P2, LCOMS, Bâtiment 308 F – CPE Lyon, 43 Boulevard du 11 Novembre 1918, F-69616 Villeurbanne, France

Received February 25, 2009

Ti(CH₂tBu)₄ (**1**) reacts selectively with the surface silanols of a silica–alumina partially dehydroxylated at 500 °C to provide the monosiloxy species [(≡SiO)Ti(CH₂tBu)₃]_{SA} (**2a**) and the bisiloxy species [(≡SiO)₂Ti(CH₂tBu)₂]_{SA} (**2b**) in a ca. 40:60 ratio, with concomitant evolution of 1.6 ± 0.2 equiv of neopentane per Ti. These surface complexes were characterized via the combined use of several techniques such as IR spectroscopy, ¹H MAS, ¹³C-CP/MAS, 2D ¹H–¹³C HETCOR, and *J*-resolved solid-state NMR, as well as mass balance analysis. By treatment under hydrogen at 150 °C the neopentyl ligands in complexes **2a,b** undergo hydrogenolysis and a mixture of supported titanium species is obtained. IR, ESR, ¹H MAS, and DQ solid-state NMR spectroscopies show the presence of ca. 3% [(≡SiO)(M_sO)TiH₂]_{SA} (**3a**; M_s = Si, Al), 5% [(≡SiO)(M_sO)Ti(Me)–H]_{SA} (**3b**), 75–80% [(≡SiO)(M_sO)₂Ti–H]_{SA} (**3c**), and 14% [(≡SiO)(M_sO)₂Ti^{III}]_{SA} (**3d**), along with (SiH_x) and (AlH_x) fragments whose formation arise from the opening of adjacent Si–O–M bridges (M = Si, Al). Species **3a–d** are efficient catalysts for the hydrogenolysis of waxes with a diesel selectivity higher than 60%. Comparison with the silica-based system shows a beneficial role of the silica–alumina support on the activity of the Ti centers, attributed to a direct interaction of the surface with the active site, which possibly facilitates the β-alkyl transfer, the key C–C bond cleavage step in the proposed mechanism.

Introduction

The low-temperature Fischer–Tropsch (F-T) process produces mainly long-chain *n*-paraffins with a wide carbon number range, up to C₁₂₀, which are virtually free of sulfur (<5 ppm) and have low aromatic contents (<1 wt %).¹ These long-chain paraffins have few economically interesting applications, except as coatings or lubricants. Conversely, diesel derived from the hydrocracking of F-T waxes with a cetane number of about 70 can be used as a blending stock in upgrading lower quality diesel, considering that a minimum cetane number of 51 is usually required for conventional commercial fuels.² Hydrocracking catalysts based on noble and group 8 metals supported on zeolites or various other supports have been developed and extensively studied;³ amorphous silica–alumina has attracted considerable interest since, with such a support, higher diesel selectivities were obtained than when using zeolite supports.⁴ For

example, high diesel selectivities were obtained over Pt/SiO₂–Al₂O₃ (SA) during the hydroprocessing of F-T waxes, and this was attributed to the mild Brønsted acidity, high surface area, and pore size distribution of the support.⁵ These metal/acid bifunctional catalysts, which are also used for alkane isomerization,^{6–8} follow the carbenium ion mechanism by (i) dehydrogenation of the alkanes on the metal sites, (ii) isomerization and cracking of olefins on the acidic sites, and (iii) hydrogenation of new olefins on the metal.⁹ However, the reported hydrocracking catalysts are efficient only at high temperatures, thus increasing the deactivation by coke formation and poisoning of the acidic sites.¹⁰ Therefore, it appears interesting to develop new hydrocracking catalysts running at low temperature and pressure and leading to an environmentally friendly process (no H₂S in the tail gas).

We and others have reported the preparation and properties of well-defined silica-supported group 4 metal hydrides

*To whom correspondence should be addressed. Tel: +33 - 4 72 43 17 94. Fax: +33 - 4 72 43 17 95. E-mail: demallmann@cpe.fr (A.d.M.); basset@cpe.fr (J.-M.B.).

(1) Dry, M. E. *Appl. Catal.*, A **1999**, 189, 185–190.
(2) De Haan, R.; Joost, G.; Mokoena, E.; Nicolaides, C. P. *Appl. Catal.*, A: *Gen.* **2007**, 327, 247–254.
(3) Leckel, D.; Liwanga-Ehumbu, M. *Energy Fuels* **2006**, 20, 2330–2336.
(4) Leckel, D. *Ind. Eng. Chem. Res.* **2007**, 46, 3505–3512.

(5) Calemma, V.; Peratello, S.; Pavoni, S.; Clerici, G.; Perego, C. *Stud. Surf. Sci. Catal.* **2001**, 136, 307–312 (Natural Gas Conversion VI).
(6) Sinfelt, J. H.; Hurwitz, H.; Rohrer, J. C. *J. Catal.* **1962**, 1, 481–483.
(7) Kouwenhoven, H. W.; van Zijll Langhout, W. C. *Chem. Eng. Prog.* **1971**, 67, 65.
(8) Vaudagna, S. R.; Comelli, R. A.; Canavese, S. A.; Figoli, N. S. *J. Catal.* **1997**, 169, 389–393.
(9) Martens, J. A.; Jacobs, P. A.; Weitkamp, J. *Appl. Catal.*, A **1986**, 20, 239–281.
(10) Stöcker, M. *Microporous Mesoporous Mater.* **2005**, 82, 257–292.

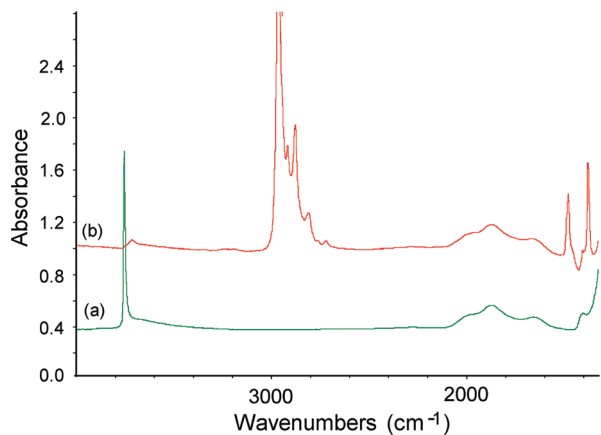
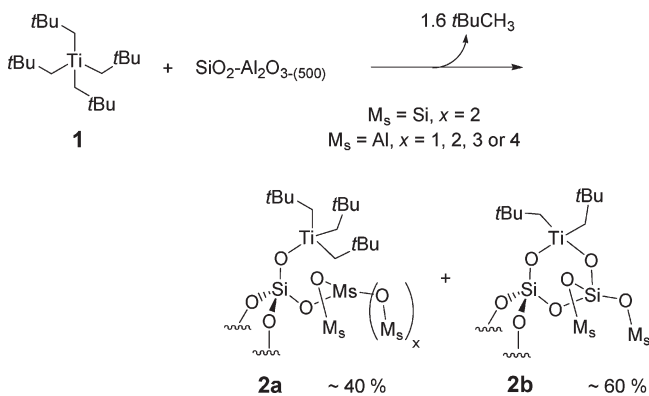


Figure 1. Monitoring the reaction of $[\text{Ti}(\text{CH}_2t\text{Bu})_4]$ and $\text{SiO}_2\text{-Al}_2\text{O}_3\text{-(500)}$ by IR spectroscopy: (a) $\text{SiO}_2\text{-Al}_2\text{O}_3\text{-(500)}$; (b) $[(\equiv\text{SiO})_x\text{Ti}(\text{CH}_2t\text{Bu})_{4-x}]_{\text{SA}}$ supported on $\text{SiO}_2\text{-Al}_2\text{O}_3\text{-(500)}$.

Scheme 1. Reaction of 1 with $\text{SiO}_2\text{-Al}_2\text{O}_3\text{-(500)}$



as $(\equiv\text{SiO})_3\text{MH}$ ($\text{M} = \text{Ti}, \text{Zr}, \text{Hf}$)^{11–20} which are able to catalyze the hydrogenolysis of alkanes under mild conditions. For example, $(\equiv\text{SiO})_3\text{ZrH}$, which is very electrophilic, can cleave the C–C bonds of propane, butanes, and pentanes (but not ethane) under a moderate hydrogen pressure (< 1 atm) and at mild temperatures (typically 25–150 °C).^{21,22} Silica–alumina-supported zirconium hydride has also been used to cleave the C–C bonds of polyolefins. The mechanism of such C–C bond cleavage was proposed to involve as a key

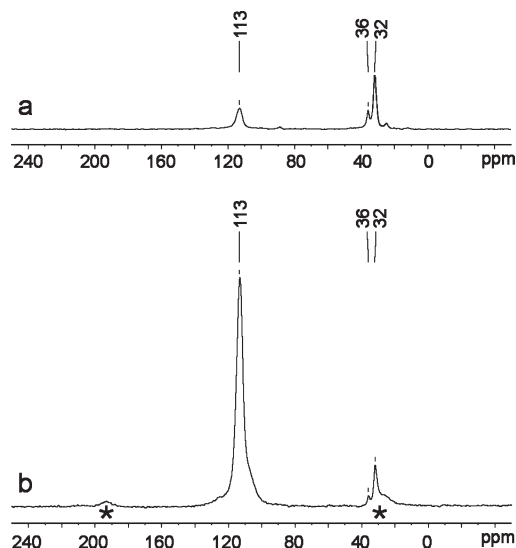


Figure 2. ^{13}C CP/MAS solid-state NMR spectra of **2a,b** (40 000 scans, recycle delay 1 s, contact time 1 ms, line broadening applied 50 Hz): (a) 0% ^{13}C -enriched **2a,b**; (b) 30% ^{13}C -enriched **2a*,b*** (two broad spinning sidebands corresponding to the 113 ppm signal are denoted with stars).

step a β -alkyl transfer, the microscopic reverse of a C=C insertion into a metal–carbon bond.²³ Due to their inherent electrophilicity, titanium complexes are good candidates for the catalytic hydrocracking of F-T waxes. Herein, we report the grafting of $[\text{Ti}(\text{CH}_2t\text{Bu})_4]$ (**1**) and the characterization of the supported complexes on silica–alumina (SA), as well as the preparation and characterization of the hydrides resulting from the hydrogenolysis of the grafted species. The activity of these silica–alumina-supported species in the hydrogenolysis of F-T waxes under a moderate hydrogen pressure (1 atm) and mild reaction temperature (typically 180 °C) has been investigated along with the previously reported silica-supported analogue.¹⁸

Results and Discussion

Grafting of $[\text{Ti}(\text{CH}_2t\text{Bu})_4]$ (1**) on Silica–Alumina. In Situ IR Study.** Silica–alumina was pressed into a self-supporting disk, and after calcination under air and treatment under vacuum at 500 °C (SA or $\text{SiO}_2\text{-Al}_2\text{O}_3\text{-(500)}$), the major surface functional groups were $\equiv\text{SiOH}$ and Lewis acid centers, while no $\text{Al}_5\text{-OH}$ surface species were observed (Figure 1a).²⁴ The sublimation of $[\text{Ti}(\text{CH}_2t\text{Bu})_4]$ (**1**) on $\text{SiO}_2\text{-Al}_2\text{O}_3\text{-(500)}$ was then monitored by in situ IR spectroscopy. The disk turned yellow, and the IR band assigned to isolated silanol groups ($\nu(\text{SiO-H})$) at 3747 cm^{-1} disappeared (Figure 1b), while a broad band centered at 3700 cm^{-1} appeared, in agreement with the presence of unreacted silanols in interaction with the adjacent grafted organometallic moieties.^{25,26} Two groups of bands concomitantly appeared in the $3000\text{--}2700$ and $1500\text{--}1300\text{ cm}^{-1}$ regions, which are respectively assigned to $\nu(\text{CH})$ and $\delta(\text{CH})$ vibrations

(11) Zakharov, V. A.; Dudchenko, V. K.; Paukshtis, E. A.; Karakchiev, L. G.; Yermakov, Y. I. *J. Mol. Catal.* **1977**, *2*, 421–435.

(12) Quignard, F.; Choplin, A.; Basset, J. M. *J. Chem. Soc., Chem. Commun.* **1991**, 1589–1590.

(13) Lecuyer, C.; Quignard, F.; Choplin, A.; Olivier, D.; Basset, J. M. *Angew. Chem., Int. Ed. Engl.* **1991**, *30*, 1660–1661.

(14) Quignard, F.; Lecuyer, C.; Bougault, C.; Lefebvre, F.; Choplin, A.; Olivier, D.; Basset, J. M. *Inorg. Chem.* **1992**, *31*, 928–930.

(15) Quignard, F.; Lecuyer, C.; Choplin, A.; Olivier, D.; Basset, J. M. *J. Mol. Catal.* **1992**, *74*, 353–363.

(16) Schwartz, J.; Ward, M. D. *J. Mol. Catal.* **1980**, *8*, 465–469.

(17) Scott, S. L.; Basset, J. M.; Nicolai, G. P.; Santini, C. C.; Candy, J. P.; Lecuyer, C.; Quignard, F.; Choplin, A. *New J. Chem.* **1994**, *18*, 115–122.

(18) Rosier, C.; Nicolai, G. P.; Basset, J. M. *J. Am. Chem. Soc.* **1997**, *119*, 12408–12409.

(19) Dornelas, L.; Reyes, S.; Quignard, F.; Choplin, A.; Basset, J. M. *Chem. Lett.* **1993**, 1931–1934.

(20) Tosin, G.; Santini, C. C.; Baudoin, A.; de Mallmann, A.; Fiddy, S.; Dablemont, C.; Basset, J. M. *Organometallics* **2007**, *26*, 4118–4127.

(21) Corker, J.; Lefebvre, F.; Lecuyer, C.; Dufaud, V.; Quignard, F.; Choplin, A.; Evans, J.; Basset, J. M. *Science* **1996**, *271*, 966–969.

(22) Lefebvre, F.; Thivolle-Cazat, J.; Dufaud, V.; Nicolai, G. P.; Basset, J. M. *Appl. Catal., A* **1999**, *182*, 1–8.

(23) Dufaud, V. R.; Basset, J. M. *Angew. Chem., Int. Ed.* **1998**, *37*, 806–810.

(24) Gora-Marek, K.; Derewinski, M.; Sarv, P.; Datka, J. *Catal. Today* **2005**, *101*, 131–138.

(25) Nedež, C.; Theolier, A.; Lefebvre, F.; Choplin, A.; Basset, J. M.; Joly, J. F. *J. Am. Chem. Soc.* **1993**, *115*, 722–729.

(26) de Mallmann, A.; Lot, O.; Perrier, N.; Lefebvre, F.; Santini, C. C.; Basset, J. M. *Organometallics* **1998**, *17*, 1031–1043.

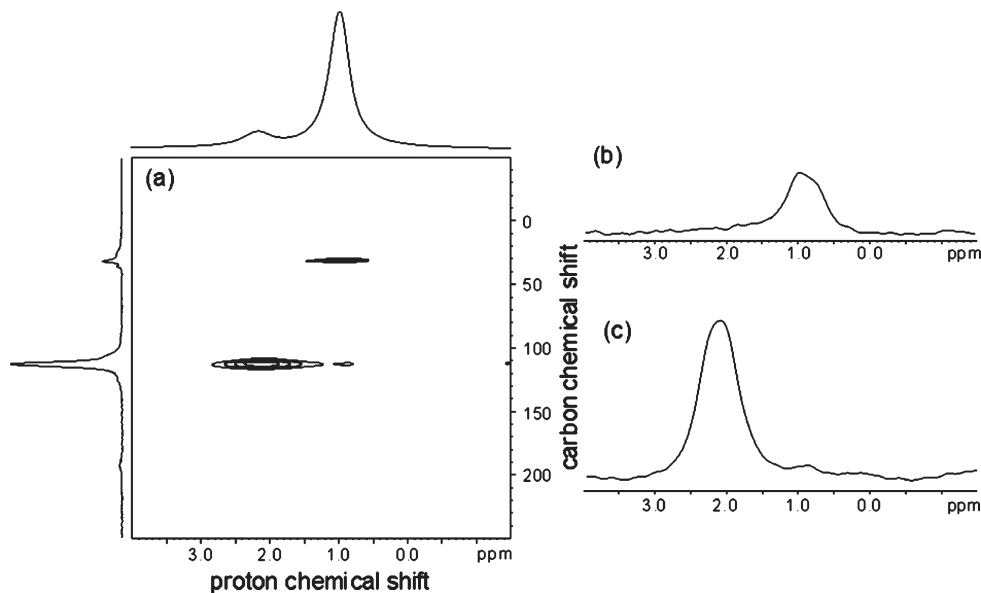


Figure 3. (a) ^1H – ^{13}C HETCOR spectrum of solid **2a***,**b*** and traces perpendicular to F2 at (b) 32 ppm and (c) 113 ppm. The spectra were recorded with 4096 scans, a relaxation delay of 1 s, and a CP contact time of 1 ms. An exponential line broadening of 50 Hz was applied before Fourier transform.

of neopentyl ligands. The irreversible disappearance of the free silanol band and the appearance of $\nu(\text{CH})$ and $\delta(\text{CH})$ bands as well as the evolution of 2,2-dimethylpropane in the gas phase is in full agreement with a chemical grafting of **1** and the formation of a $\equiv\text{SiOTi}$ bond, as was observed for the grafting of **1** on partly dehydroxylated silica or MCM-41.²⁷

Mass Balance Analyses. $[\text{Ti}(\text{CH}_2t\text{Bu})_4]$ (**1**) in pentane solution was allowed to react at 25 °C for 4 h with $\text{SiO}_2\text{--Al}_2\text{O}_3\text{-(500)}$ as a powder (1.4 OH/nm²; 0.91 mmol/g), followed by filtration, three washing cycles with pentane, and drying under vacuum at 25 °C to give a yellow solid, **2**. A Ti loading of 2.4–2.9 wt % was obtained according to elemental analysis, corresponding to 0.50–0.62 mmol Ti/g. During grafting 1.4–1.8 equiv of $t\text{BuCH}_3/\text{Ti}$ evolved, and the resulting solid contained 11.9–12.4 C/Ti, according to elemental analyses; these analytical results are consistent with the formation of the two surface species $[\equiv\text{SiOTi}(\text{CH}_2t\text{Bu})_3]_{\text{SA}}$ (**2a**) and $[(\equiv\text{SiO})_2\text{Ti}(\text{CH}_2t\text{Bu})_2]_{\text{SA}}$ (**2b**), in a ratio close to 40:60 (Scheme 1).

Solid-State NMR Spectroscopy. The ^1H MAS solid-state NMR spectrum of solid **2** exhibits only two signals (Figure S1, Supporting Information), which were assigned by comparison with the signals of the monopodal species $[(\equiv\text{SiO})\text{Ti}(\text{CH}_2t\text{Bu})_3]_{\text{S}}$ and bipodal species $[(\equiv\text{SiO})_2\text{Ti}(\text{CH}_2t\text{Bu})_2]_{\text{S}}$, prepared by reaction of $[\text{Ti}(\text{CH}_2t\text{Bu})_4]$ with $\text{SiO}_2\text{-(700)}$ and MCM-41₍₂₀₀₎, respectively.²⁷ The first signal at 1.2 ppm corresponds to the methyl resonances of the $-\text{CH}_2\text{C}(\text{CH}_3)_3$ fragments and the second at 2.4 ppm is attributed to the methylene protons $-\text{CH}_2\text{CMe}_3$. The ^{13}C CP/MAS solid-state NMR spectrum (Figure 2a) shows an intense peak at 32 ppm assigned to the methyl groups $-\text{CH}_2\text{C}(\text{CH}_3)_3$ and two weaker signals at 36 and 113 ppm, corresponding to the quaternary carbon $-\text{CH}_2\text{CMe}_3$ and the methylenic carbons of a neopentyl ligand $-\text{CH}_2\text{CMe}_3$, respectively. In order to obtain better quality ^{13}C NMR spectra, the complex $[\text{Ti}(*\text{CH}_2t\text{Bu})_4]$ (**1***), 30% ^{13}C -enriched

on the carbons directly bound to the titanium center, was prepared and grafted on $\text{SiO}_2\text{--Al}_2\text{O}_3\text{-(500)}$. While the ^1H MAS spectra of $[\equiv\text{SiOTi}(*\text{CH}_2t\text{Bu})_3]_{\text{SA}}$ (**2a***) and $[(\equiv\text{SiO})_2\text{Ti}(*\text{CH}_2t\text{Bu})_2]_{\text{SA}}$ (**2b***) are identical with those of **2a,b**, the ^{13}C CP/MAS spectrum shows again the signals at 32, 36, and 113 ppm (Figure 2b), but the intensity of the 113 ppm signal dramatically increases, which is consistent with its assignment to the carbon directly attached to the metal: i.e., $\text{Ti}^*\text{--CH}_2t\text{Bu}$. Moreover, the assignments are confirmed by 2D ^1H – ^{13}C heteronuclear correlation (HETCOR) spectroscopy, for which short contact times (1 ms) have been chosen in order to detect only the protons directly attached to a carbon. Under these conditions, the 2D HETCOR spectrum of **2a***,**b*** shows two strong correlations between proton and carbon signals ($\delta(^1\text{H})/\delta(^{13}\text{C})$) 1.2/32 and 2.4/113 (Figure 3a), but no correlation is observed for the ^{13}C signals at 36 ppm, consistent with its assignment to quaternary carbons. Both correlations at 1.2/32 and 2.4/113 corroborate their respective attributions to the methyl ($-\text{CH}_2\text{C}(\text{CH}_3)_3$; traces in Figure 3b) and methylene groups ($-\text{CH}_2t\text{Bu}$; traces in Figure 3c) of the neopentyl ligands. Finally, J -resolved 2D solid-state NMR spectroscopy applied to **2a***,**b*** (Figure 4) shows a quadruplet ($^1J_{\text{CH}} = 114$ Hz) at 32 ppm fully consistent with its assignments to the methyl of the $t\text{Bu}$ groups (trace in Figure 4b); the singlet at 36 ppm fits well with the quaternary carbon of the $t\text{Bu}$ groups (trace in Figure 4c),^{28–31} while the triplet ($^1J_{\text{CH}} = 107$ Hz) at 113 ppm is in agreement with the methylenic carbon of the neopentyl fragment (trace in Figure 4d).

In summary, the reaction of $[\text{Ti}(\text{CH}_2t\text{Bu})_4]$ (**1**) with $\text{SiO}_2\text{--Al}_2\text{O}_3\text{-(500)}$ leads to the formation of the two surface

(28) Terao, T.; Miura, H.; Saika, A. *J. Am. Chem. Soc.* **1982**, *104*, 5228–5229.

(29) Mayne, C. L.; Pugmire, R. J.; Grant, D. M. *J. Magn. Reson.* **1984**, *56*, 151–153.

(30) Miura, H.; Terao, T.; Saika, A. *J. Magn. Reson.* **1986**, *68*, 593–596.

(31) Lesage, A.; Steuernagel, S.; Emsley, L. *J. Am. Chem. Soc.* **1998**, *120*, 7095–7100.

(27) Bini, F.; Rosier, C.; Saint-Arroman, R. P.; Neumann, E.; Dablemont, C.; de Mallmann, A.; Lefebvre, F.; Niccolai, G. P.; Basset, J. M.; Crocker, M.; Buijink, J. K. *Organometallics* **2006**, *25*, 3743–3760.

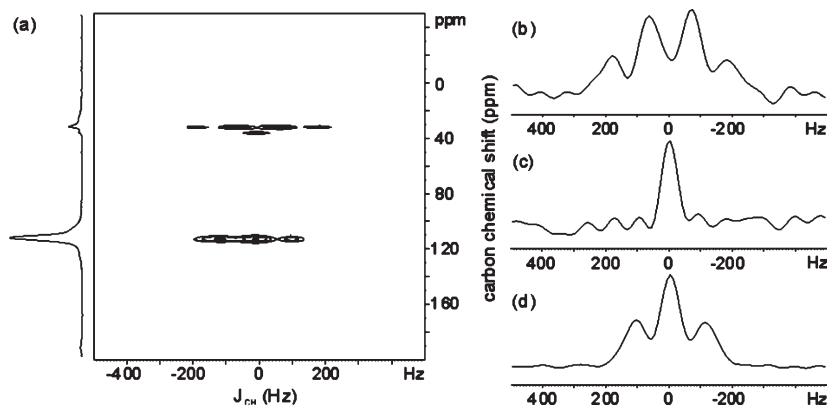


Figure 4. (a) 2D J -resolved solid-state NMR spectrum of the solid $2a^*, b^*$, 30% ^{13}C -enriched at the α -positions (*) and traces extracted along the ω_1 dimension of the 2D J -resolved spectrum at the carbon chemical shift frequencies (b) 32 ppm, (c) 36 ppm, and (d) 113 ppm. The spectra were recorded with 1024 scans, a relaxation delay of 2 s, and a CP contact time of 2 ms.

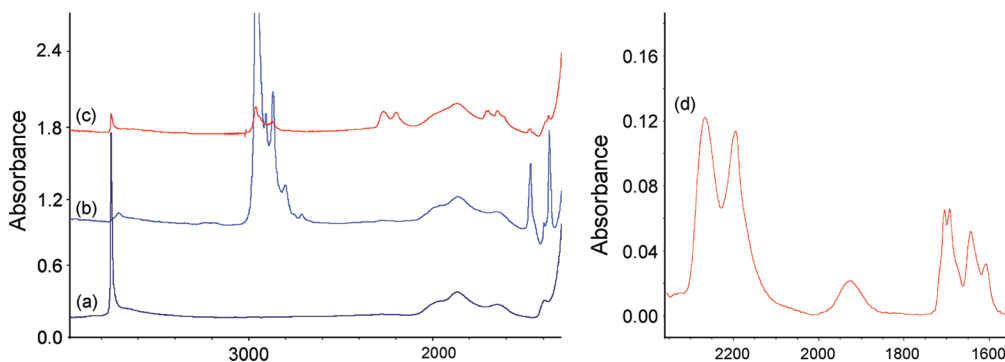


Figure 5. Monitoring the formation of titanium hydrides supported on $\text{SiO}_2\text{-Al}_2\text{O}_{3-(500)}$ (**3a–c**) by IR spectroscopy: (a) silica–alumina dehydroxylated at 500 °C; (b) $[(\equiv\text{SiO})\text{Ti}(\text{CH}_2t\text{Bu})_3]_{\text{SA}}$ and $[(\equiv\text{SiO})_2\text{Ti}(\text{CH}_2t\text{Bu})_2]_{\text{SA}}$; (c) after treatment under H_2 at 150 °C for 4 h; (d) subtraction (c)–(a), zoom of the 2300–1500 cm^{-1} region.

species $[(\equiv\text{SiO}-\text{Ti}(\text{CH}_2t\text{Bu})_3]_{\text{SA}}$ (**2a**) and $[(\equiv\text{SiO})_2\text{Ti}(\text{CH}_2t\text{Bu})_2]_{\text{SA}}$ (**2b**) (Scheme 1) in a ratio close to 40:60, in which the titanium atom is grafted to the surface via one or two covalent ($\equiv\text{SiO}-\text{Ti}$) bonds, as evidenced by mass balance analysis and IR and NMR spectroscopy.

Preparation of the Titanium Hydride Supported on Silica–Alumina by Reaction of $[(\equiv\text{SiO})\text{Ti}(\text{CH}_2t\text{Bu})_3]_{\text{SA}}$ and $[(\equiv\text{SiO})_2\text{Ti}(\text{CH}_2t\text{Bu})_2]_{\text{SA}}$ with H_2 . In Situ IR Study. When $[(\equiv\text{SiO})\text{Ti}(\text{CH}_2t\text{Bu})_3]_{\text{SA}}$ (**2a**) and $[(\equiv\text{SiO})_2\text{Ti}(\text{CH}_2t\text{Bu})_2]_{\text{SA}}$ (**2b**) are heated under H_2 for 4 h at 150 °C, the yellow material darkens into a brown solid, **3**. The monitoring of the reaction by infrared spectroscopy (Figure 5) shows the disappearance of ca. 90% of the intensity of the $\nu(\text{C}-\text{H})$ and $\delta(\text{C}-\text{H})$ bands. In addition, new bands centered at 1600–1725, 1926, 2195, and 2267 cm^{-1} appear, which are assigned to $\nu(\text{TiH})$, $\nu(\text{AlH})$, and $\nu(\text{SiH})$, respectively.^{18,23} These assignments were further confirmed through the H/D exchange reaction at room temperature under D_2 (550 Torr): the intensity of vibration bands at 1600–1725 cm^{-1} decreased by ca. 90%, as expected for Ti–H (Figure S2, Supporting Information), while the $\nu(\text{Si}-\text{H})$ bands (2195 and 2267 cm^{-1}) and $\nu(\text{Al}-\text{H})$ band at 1926 cm^{-1} were not affected by this treatment, as expected for silicon and aluminum hydrides. During the hydrogenolysis process, a band of weak intensity also reappeared at 3747 cm^{-1} corresponding to isolated silanols, which were probably in interaction with the alkyl ligands (vide supra, $\nu(\text{OH})$ band at 3700 cm^{-1}) and became free when these ligands underwent hydrogenolysis. Simultaneously, methane (9 equiv of CH_4/Ti) and ethane (1.1 equiv of $\text{C}_2\text{H}_6/\text{Ti}$) were observed in the gas phase as the products

resulting from the hydrogenolysis of the neopentyl ligands, which corresponds to 11.2 ± 1.3 equiv of C/Ti.

ESR and Solid-State NMR Spectroscopy. Samples of solid **3**, prepared by impregnation on silica–alumina powder and further hydrogenolysis, were analyzed by ESR and ^1H NMR spectroscopy. While the former technique points out the presence of ca. 14% of Ti^{III} species in solid **3**, after a double integration of the characteristic signal at 3439 G (Figure S3, Supporting Information), the latter gives additional information: the ^1H NMR spectrum of **3** displays several signals at 0.9, 1.3, 1.8 (shoulder), 4.4, and 8.6 ppm (Figure 6a). First, the signals at 0.9 and 1.3 ppm can be assigned to residual alkyl fragments, which did not undergo full hydrogenolysis. Second, the signal at 1.8 ppm is consistent with residual silanols, while the signal at 4.4 ppm can be readily assigned to $(\equiv\text{Si}-\text{H})$ protons.^{32,33} Finally, the quite broad downfield signal at 8.6 ppm can be attributed to a surface titanium hydride, in agreement with a previous assignment of a resonance at 8.5 ppm to the hydride ligand of the molecular complex $\{(\text{ArO})_3\text{Ti}-\text{H}\cdot\text{PMe}_3\}$.³⁴ The deconvolution³⁵ of this broad signal between 7 and 10 ppm shows two

(32) Campbell-Ferguson, H. J.; Ebsworth, E. A. V.; MacDiarmid, A. G.; Yoshioka, T. *J. Phys. Chem.* **1967**, *71*, 723.

(33) Soignier, S.; Taoufik, M.; Le Roux, E.; Saggio, G.; Dablemont, C.; Baudouin, A.; Lefebvre, F.; de Mallmann, A.; Thivolle-Cazat, J.; Basset, J. M.; Sunley, G.; Maunders, B. M. *Organometallics* **2006**, *25*, 1569–1577.

(34) Noth, H.; Schmidt, M. *Organometallics* **1995**, *14*, 4601–4610.

(35) Massiot, D.; Fayon, F.; Capron, M.; King, I.; Le Calve, S.; Alonso, B.; Durand, J. O.; Bujoli, B.; Gan, Z. H.; Hoatson, G. *Magn. Reson. Chem.* **2002**, *40*, 70–76.

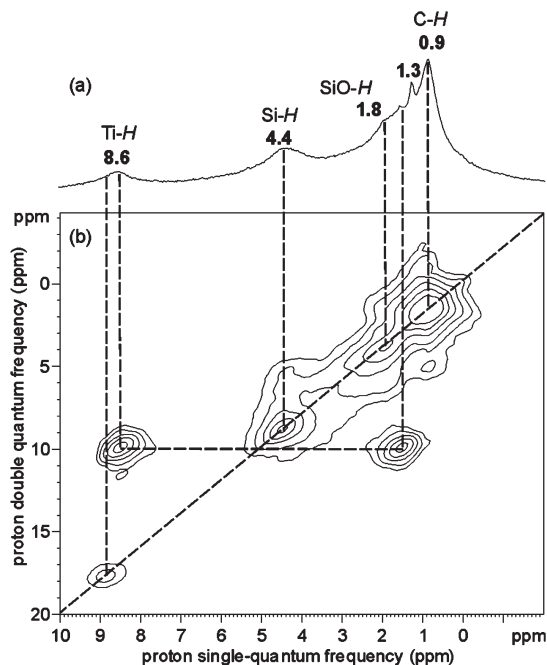


Figure 6. (a) ^1H MAS solid-state NMR spectrum of $[\text{Ti-H}]$ species obtained as indicated in Scheme 2. (b) DQ rotor-synchronized 2D ^1H MAS spectrum of $[\text{Ti-H}]$ species (see text and Experimental Section for more details).

different peaks centered at 8.6 and 9.1 ppm in a ca. 92:8 ratio (Figure S4, Supporting Information). In contrast to IR spectroscopy, the ^1H MAS NMR spectrum of the surface species does not show a resonance indicating the presence of Al-H species (expected at ca. 4–5 ppm³⁶), probably due to the broadness of the signal induced by the quadrupolar moment of trigonal Al centers. To further assign these various signals, 2D multiple-quantum (MQ) proton spectroscopy under magic angle spinning (MAS) was applied. To probe structural information inherent to proton–proton dipolar couplings, the ^1H DQ MAS spectrum was recorded for $[\text{Ti-H}]$ at a MAS frequency of ca. 10 kHz (Figure 6b). In this experiment, the evolution of the DQ coherence created between a pair of dipolar-coupled protons is observed during the indirect detection time t_1 . The DQ frequency in the ω_1 dimension corresponds to the sum of the two single quantum frequencies of the two coupled protons and correlates in the ω_2 dimension with the two corresponding proton resonances. Therefore, the observation of a DQ cross-peak implies a close proximity between the two protons involved in this correlation. Autocorrelation peaks are observed on the diagonal of the 2D spectrum (Figure 6b), in particular for the alkyl protons at 0.9 ppm (ca. 2 ppm in the ω_1 dimension, for CH_2 , with $z=2, 3$), for the remaining OH groups at 1.8 ppm (ca. 3.7 ppm in the ω_1 dimension, probably for geminal $>\text{Si}(\text{OH})_2$ silanols), and for the signal attributed to $(\equiv\text{Si-H})$ protons resonances at 4.4 ppm (8.8 ppm in the ω_1 dimension), showing the presence of silicon dihydride $[(\text{M}_s\text{O})_2\text{SiH}_2]$. A weak autocorrelation peak is also observed for a proton resonance at ca. 8.9 ppm (17.8 ppm in the ω_1 dimension), which unambiguously allows the assignment of this resonance to a titanium dihydride, $[(\equiv\text{SiO})(\text{M}_s\text{O})\text{TiH}_2]_{\text{SA}}$ (**3a**; $\text{M}_s = \text{Si, Al}$; see Scheme 2), as was

found previously in the case of zirconium surface organometallic chemistry, where $[(\equiv\text{SiO})_2\text{ZrH}_2]$ species were similarly characterized.³⁷ The proton resonance at 8.6 ppm does not show such an autocorrelation and can then be attributed to monohydride species, which can be described by the general formula $[(\equiv\text{SiO})(\text{M}_s\text{O})_{2-x}(\text{R})_x\text{Ti-H}]_{\text{SA}}$ ($x = 0, 1, 2$; $\text{M}_s = \text{Si, Al}$; $\text{R} =$ alkyl group, including CH_3). The two signals revealed upon the deconvolution of the total broad titanium hydride resonance could then be attributed to a few dihydride species, $[(\equiv\text{SiO})(\text{M}_s\text{O})\text{TiH}_2]_{\text{SA}}$ (**3a**), around 9 ppm and to monohydride species, $[(\equiv\text{SiO})(\text{M}_s\text{O})_{2-x}(\text{R})_x\text{Ti-H}]_{\text{SA}}$, at 8.6 ppm. In addition, a clear correlation is observed between the resonance at 8.6 ppm and a part of a signal at ca. 1.6 ppm (cross-peaks at ca. 10 ppm in the ω_1 dimension in Figure 6). This may correspond to a correlation between the proton of the monohydride species $[(\equiv\text{SiO})(\text{M}_s\text{O})_{2-x}(\text{R})_x\text{Ti-H}]_{\text{SA}}$ ($x = 0, 1, 2$) and either residual OH groups located in the vicinity of the $\equiv\text{Ti-H}$ group but too far to react with it or residual alkyl groups bound to titanium ($x = 1, 2$). The precise nature and amount of the different hydride and Ti^{III} species supported on solid **3** could be finally obtained from the double integration of the ESR signal, from the integration of the ^1H MAS NMR signals associated with di- and monohydrides, and from the butanolysis³⁸ of sample **3**.

In conclusion, according to the previously described methods, the treatment under H_2 at 150 °C of the mixture of $[(\equiv\text{SiO})\text{Ti}(\text{CH}_2t\text{Bu})_3]_{\text{SA}}$ (**2a**) and $[(\equiv\text{SiO})_2\text{Ti}(\text{CH}_2t\text{Bu})_2]_{\text{SA}}$ (**2b**) leads to new surface titanium species: $[(\equiv\text{SiO})(\text{M}_s\text{O})\text{TiH}_2]_{\text{SA}}$ (**3a**) $[(\equiv\text{SiO})(\text{M}_s\text{O})(\text{Me})\text{Ti-H}]_{\text{SA}}$ (**3b**), $[(\equiv\text{SiO})(\text{M}_s\text{O})_2\text{Ti-H}]_{\text{SA}}$ (**3c**), and $[(\equiv\text{SiO})(\text{M}_s\text{O})_2\text{Ti}^{\text{III}}]_{\text{SA}}$ (**3d**). However, complexes $[(\equiv\text{SiO})\text{Ti}(\text{CH}_2t\text{Bu})_3]_{\text{SA}}$ (**2a**) and $[(\equiv\text{SiO})_2\text{Ti}(\text{CH}_2t\text{Bu})_2]_{\text{SA}}$ (**2b**) were expected to lead to trishydride and dihydride (**3a**) species, respectively, by hydrogenolysis of the titanium–carbon bonds. However, since silica–alumina is amorphous, the various titanium surface species, initially **2a**, **b**, are surrounded by different local environments: that is, different types of Si–O–Si and Si–O–Al bridges formed during the dehydroxylation step. For that reason and as already observed with other metal and oxide supports,^{15,21,33,39} the hydrogenolysis of $[(\equiv\text{SiO})\text{Ti}(\text{CH}_2t\text{Bu})_3]_{\text{SA}}$ (**2a**) generates first $[(\equiv\text{SiO})(\text{M}_s\text{O})\text{TiH}_2]_{\text{SA}}$ (**3a**) and $[(\equiv\text{SiO})(\text{M}_s\text{O})(\text{Me})\text{Ti-H}]_{\text{SA}}$ (**3b**; $\text{M}_s = \text{Si, Al}$), together with $[\text{Si-H}]$ and $[\text{Al-H}]$ surface species via the opening of neighboring Si–O–Si and Si–O–Al bridges and the transfer of an hydride from the metal to a Si or Al surface atom (Scheme 2). Then, in most cases, other Si–O–Si or Si–O–Al bridges are close enough to the titanium centers to allow the surface complex $[(\equiv\text{SiO})(\text{M}_s\text{O})\text{TiH}_2]_{\text{SA}}$ (**3a**) to react further and yield the major monohydride species $[(\equiv\text{SiO})(\text{M}_s\text{O})_2\text{Ti-H}]_{\text{SA}}$ (**3c**) as 75–80% of the surface titanium species observed by ESR and ^1H NMR, leaving only ca. 3% of the dihydride species $[(\equiv\text{SiO})(\text{M}_s\text{O})\text{TiH}_2]_{\text{SA}}$ (**3a**). The other monohydride complex $[(\equiv\text{SiO})(\text{M}_s\text{O})(\text{Me})\text{Ti-H}]_{\text{SA}}$ (**3b**) would account for less than

(36) Uhl, W.; Jana, B. *Chem. Eur. J.* **2008**, *14*, 3067–3071.

(37) Rataboul, F.; Baudouin, A.; Thieuleux, C.; Veyre, L.; Coperet, C.; Thivolle-Cazat, J.; Basset, J. M.; Lesage, A.; Emsley, L. *J. Am. Chem. Soc.* **2004**, *126*, 12541–12550.

(38) The butanolysis consisted of the treatment of sample **3** with *tert*-butyl alcohol (40 mbar) for 1 h at 30 °C, followed by evacuation at 80 °C for 2 h. During this treatment, titanium hydrides disappeared while surface $\equiv\text{Ti}^{\text{IV}}\text{Bu}$ species appeared, with the concomitant evolution of dihydrogen ($\text{H}_2/\text{Ti} = 0.85 \pm 0.15$) and a small amount of methane ($\text{CH}_4/\text{Ti} = 0.04$). This means that less than 5% of the surface titanium was present as $\equiv\text{TiMe}$ species in sample **3** and that methyl was the only alkyl ligand bound to Ti. The main monohydride Ti species are then $[(\equiv\text{SiO})(\text{M}_s\text{O})(\text{Me})\text{Ti-H}]$ (**3b**) and $[(\equiv\text{SiO})(\text{M}_s\text{O})_2\text{Ti-H}]$ (**3c**), representing respectively less than 5% and 75–80% of the surface Ti species. After butanolysis, the ESR signal characteristic of Ti^{III} species decreased from 14% to 3% of the total Ti content.

(39) Vidal, V.; Theolier, A.; Thivolle-Cazat, J.; Basset, J. M.; Corker, J. *J. Am. Chem. Soc.* **1996**, *118*, 4595–4602.

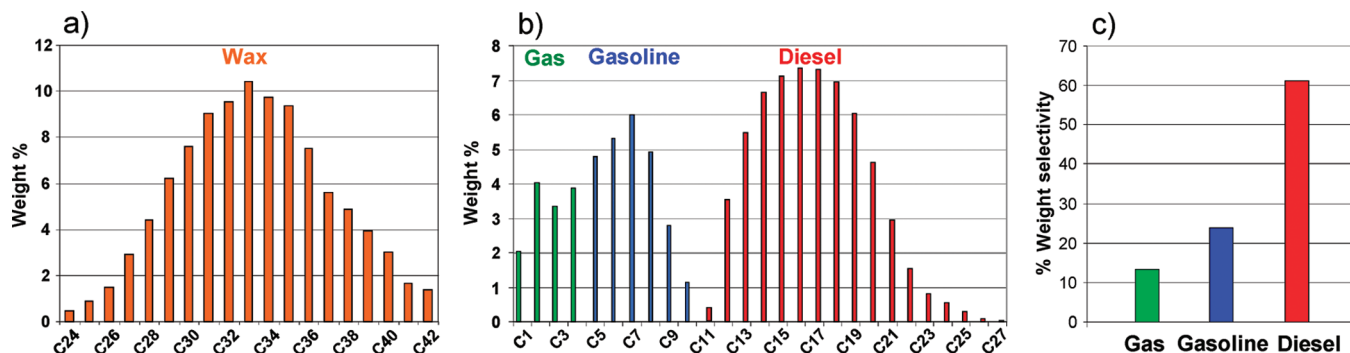
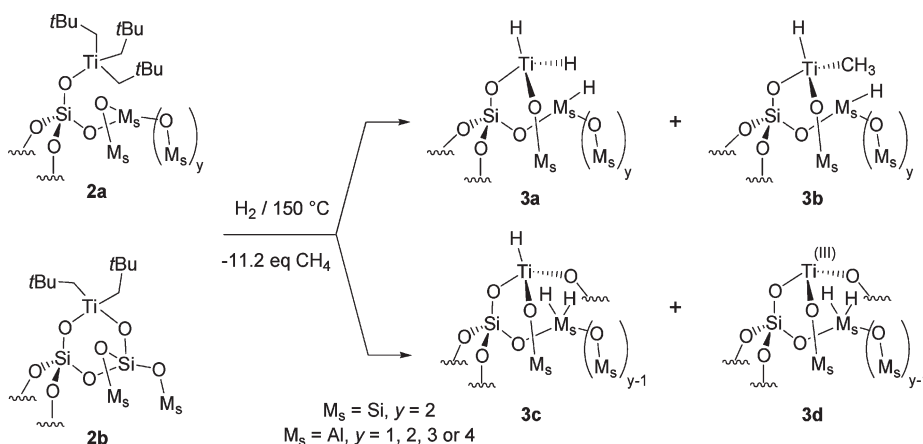


Figure 7. Hydrogenolysis of a paraffin wax catalyzed by $[\text{Ti-H}]/\text{SiO}_2\text{-Al}_2\text{O}_3$ (1 bar of H_2 , 180°C): (a) initial hydrocarbon weight distribution of the wax; (b) hydrocarbon weight distribution obtained after the hydrogenolysis reaction (the decay observed between C8 and C13 is likely due to an analytical artifact: only 92% of the products could be detected by GC with our procedure); (c) weight distribution of the categorized products obtained after hydrogenolysis.

Scheme 2. Main Structures Proposed for Titanium Hydrides Supported on Silica–Alumina



5% of the surface titanium. In addition to this main process, $[(\equiv\text{SiO})(\text{MsO})_2\text{Ti}^{\text{III}}]_{\text{SA}}$ (**3d**) surface species are also formed, accounting for ca. 14% of the observed surface titanium.

Activity in the Hydrogenolysis of FT Waxes. The titanium hydrides on silica–alumina **3** and titanium hydrides on silica¹⁸ dehydroxylated at 500°C were tested in the reaction of wax hydrogenolysis, in order to study the effect of the support on the activity and selectivity; a low-molecular-weight wax (C20–C50, Figure 7a) obtained from Aldrich was used in a semicontinuous flow reactor at 180°C under a hydrogen stream (1 atm, 20 mL/min; see the Experimental Section and Figure S5 in the Supporting Information). As can be seen in Table 1, after 24 h the conversion of the wax obtained with titanium hydrides supported on silica–alumina, **3**, is complete, while under similar conditions the conversion is only 30% with titanium hydrides supported on silica, $[\text{Ti-H}]_{\text{SiO}_2}$. Interestingly, solid **3** leads to a higher diesel selectivity (63%) compared to titanium hydride on silica (40%), whereas this latter produces more C1–C2 hydrocarbons (24%) and both catalysts show similar selectivities in C3–C4 or C5–C9 products (Figure 7b,c). In order to determine the beneficial role of the silica–alumina support, another experiment was carried out by adding 200 mg of pure $\text{SiO}_2\text{-Al}_2\text{O}_3(500)$ to $[\text{Ti-H}]_{\text{SiO}_2}$, under the same experimental conditions. The results show that the activity is the same as that for $[\text{Ti-H}]_{\text{SiO}_2}$; the wax conversion was 34% instead of 30%, but with the formation of a more important proportion of gaseous C1–C4 products, ca. 56% instead of 33%, and of a lower diesel fraction (selectivities: C1–C2, 40%; C3–C4, 16%; C5–C9, 29%; C10–C22, 17%). The difference in selectivity between the

$[\text{Ti-H}]_{\text{SiO}_2}$ and $\{[\text{Ti-H}]_{\text{SiO}_2} + \text{SiO}_2\text{-Al}_2\text{O}_3(500)\}$ systems can be explained by the reactivity of the Brønsted acid sites present in the pure silica–alumina₍₅₀₀₎, while they have been eliminated for $[\text{Ti-H}]_{\text{SiO}_2}$ and $[\text{Ti-H}]_{\text{SiO}_2\text{-Al}_2\text{O}_3}$ by the grafting reaction of $\text{Ti}(\text{CH}_2\text{tBu})_4$ on the OH groups of the surface. Indeed, under the same conditions, a blank experiment with silica–alumina₍₅₀₀₎ alone gave a very low wax conversion of ca. 3% and produced only C1–C4 gaseous products. Since the activity observed for the $\{[\text{Ti-H}]_{\text{SiO}_2} + \text{SiO}_2\text{-Al}_2\text{O}_3(500)\}$ system is still much lower than that obtained with $[\text{Ti-H}]_{\text{SiO}_2\text{-Al}_2\text{O}_3}$, it thus seems that a direct interaction of the surface with the active site is responsible for the change in reactivity observed for $[\text{Ti-H}]_{\text{SiO}_2\text{-Al}_2\text{O}_3}$ compared to $[\text{Ti-H}]_{\text{SiO}_2}$, rather than the intervention of a bifunctional mechanism. Similar support effects have been evidenced in the field of polymerization, where it is known that alumina-supported organometallic complexes are usually more reactive than their corresponding silica equivalents,^{40–45} and this has

(40) Marks, T. J. *Acc. Chem. Res.* **1992**, *25*, 57–65.

(41) Tullock, C. W.; Tebbe, F. N.; Mulhaupt, R.; Ovenall, D. W.; Setterquist, R. A.; Ittel, S. D. *J. Polym. Sci., Part A* **1989**, *27*, 3063–3081.

(42) Ballard, D. G. H. *J. Polym. Sci., Part A* **1975**, *13*, 2191–2212; *Coord. Polym.* **1975**, 223–262.

(43) Tullock, C. W.; Mulhaupt, R.; Ittel, S. D. *Makromol. Chem. Rapid Commun.* **1989**, *10*, 19–23.

(44) Collette, J. W.; Tullock, C. W.; Macdonald, R. N.; Buck, W. H.; Su, A. C. L.; Harrell, J. R.; Mulhaupt, R.; Anderson, B. C. *Macromolecules* **1989**, *22*, 3851–3858.

(45) Jezequel, M.; Dufaud, V.; Ruiz-García, M. J.; Carrillo-Hermosilla, F.; Neugebauer, U.; Nicolai, G. P.; Lefebvre, F.; Bayard, F.; Corker, J.; Fiddy, S.; Evans, J.; Broyer, J. P.; Malinge, J.; Basset, J. M. *J. Am. Chem. Soc.* **2001**, *123*, 3520–3540.

Table 1. Hydrolysis of a Paraffin Wax^a: Comparison between Titanium Hydride (75 μ mol of Ti) Supported on Silica and Silica–Alumina

	Catalyst	
	[Ti–H] _{silica(500)}	[Ti–H] _{silica–alumina(500)}
Conversion (wt %)	30	100
C1–C2 selectivity (wt %)	24	6
C3–C4 selectivity (wt %)	9	7
C5–C9 (naphtha) selectivity (wt %)	28	24
C10–C22 (diesel) selectivity (wt %)	39	63

^aThe initial hydrocarbon weight distribution is indicated in Figure 7. Conditions: 400 mg of wax; 180 °C, P_{H_2} = 1 bar, flow rate 20 mL/min.

been often associated with the presence of cationic species favored on “acidic” alumina and not on “neutral” silica.

The mechanism proposed for such hydrogenolysis reactions involving group 4 metals is based on a key C–C bond cleavage elementary step, already known in organometallic chemistry: namely the β -alkyl transfer,²³ which is the microscopic reverse of a C=C double-bond insertion into a metal–carbon bond and would be the rate-limiting step.⁴⁶ Because of this step, the overall reaction should be thermodynamically unfavorable, except that the hydrogenation of the olefinic double bonds provides the driving force which makes the process run. In a first step, a C–H bond in the paraffinic chain is activated by the metal hydride, the metal being in a d^0 configuration, through a σ -bond metathesis with the formation of a metal–alkyl complex and liberation of dihydrogen. The second step consists of a β -alkyl transfer, leading to the formation of an olefin and a smaller alkyl group σ -coordinated to the metal. Then follows the olefin insertion into a M–H bond and hydrogenolysis of the metal–alkyl bonds to give smaller alkanes with the regeneration of the metal–hydride bonds. In the case of supported zirconium hydrides, an influence of the support has been theoretically evidenced for the β -alkyl transfer: while for a zirconium center anchored onto silica, the olefin produced after this step would be directly emitted in the gas phase, without strong interaction with the surface,⁴⁶ for zirconium sites supported on alumina, the olefin would be more strongly π -coordinated to the zirconium center, probably due to its cationic character on this support, which stabilizes the π -olefin complex.⁴⁷ This would also be the case for some titanium centers supported onto silica–alumina which would be more electrophilic than those supported onto silica, thus facilitating the further formation of the Ti–olefin π -complex in the key β -alkyl transfer step of the proposed mechanism and may explain the higher activity observed for [Ti–H]_{SiO₂–Al₂O₃} compared to [Ti–H]_{SiO₂}.

Conclusion

In conclusion, Ti(CH₂tBu)₄ (**1**) reacts selectively with the surface silanols of a silica–alumina partially dehydroxylated

at 500 °C and gives the monosiloxy species [(≡SiO)–Ti(CH₂tBu)₃]_{SA} (**2a**) and the bisiloxy species [(≡SiO)₂Ti(CH₂tBu)₂]_{SA} (**2b**) in a 40:60 ratio. These surface complexes were characterized by the combined use of several techniques such as IR spectroscopy, ¹H MAS, ¹³C-CP/MAS, 2D ¹H–¹³C HETCOR, and *J*-resolved solid-state NMR as well as mass balance analysis. By treatment under hydrogen at 150 °C the neopentyl ligands in complexes **2a,b** undergo hydrogenolysis and a mixture of supported titanium species is obtained. IR spectroscopy, ESR, ¹H MAS, and DQ solid-state NMR spectroscopy show the presence of ca. 3% [(≡SiO)(M_sO)TiH₂]_{SA} (**3a**; M_s = Si, Al), less than 5% [(≡SiO)(M_sO)(Me)Ti–H]_{SA} (**3b**), 75–80% [(≡SiO)(M_sO)₂Ti–H]_{SA} (**3c**), and 14% [(≡SiO)(M_sO)₂Ti^{III}]_{SA} (**3d**), along with (SiH_x) and (AlH_x) fragments via the opening of adjacent Si–O–M_s bridges (M_s = Si, Al). Species **3a–d** efficiently catalyze the hydrogenolysis of a paraffin wax, affording a diesel selectivity higher than 60%. Comparison with the silica-supported system has evidenced a beneficial role of the silica–alumina support on the activity of the Ti centers, attributed to a direct interaction of the surface with the active site, which possibly facilitates the β -alkyl transfer, the key C–C bond cleavage step in the proposed mechanism.

Experimental Section

General Procedure. All experiments were carried out by using standard Schlenk and glovebox techniques for the organometallic synthesis. Solvents were purified and dried according to standard procedures. C₆D₆ (SDS) was distilled over Na/benzophenone and stored over 3 Å molecular sieves. TiCl₄ (99%), 1,2-dibromoethane (99%, Aldrich), 2,2'-biquinoline (98%, Lancaster), ¹³CO₂ (99% ¹³C, Cambridge Isotopes), *t*BuMgCl (1.7 M in pentane, Aldrich), LiAlH₄ (95%, Aldrich, stored under argon), MgSO₄ (Laurylab), NaHCO₃ (Prolabo), and Vielsmeier reagent (95%, Aldrich, stored under argon) were used as received. *t*BuCH₂Li was prepared from *t*BuCH₂Cl (98%, Lancaster, used as received) and Li wire (Aldrich). [Ti(CH₂tBu)₄] was prepared according to the literature procedure.⁴⁸ Gas-phase analyses were performed on a Hewlett-Packard 5890 Series II gas chromatograph equipped with a flame ionization detector and an Al₂O₃/KCl on fused silica column (50 m × 0.32 mm).

Elemental analyses were performed at the CNRS Central Analysis Department of Solaize (metal analyses) or in the Laboratory of Prof. Dormond, LSEO of Dijon (C, H analyses). IR spectra were recorded on a Nicolet 5700 FT-IR spectrometer, using an IR cell equipped with CaF₂ windows, allowing in situ studies. Typically, 16 scans were accumulated for each spectrum (resolution 2 cm⁻¹). Solution NMR spectra were recorded on an Avance-300 Bruker spectrometer. All chemical shifts were measured relative to residual ¹H or ¹³C resonances in C₆D₆: δ 7.15 ppm for ¹H and 128 ppm for ¹³C.

¹H MAS and ¹³C CP-MAS Solid-State NMR Spectra. These spectra were recorded on a Bruker Avance-500 spectrometer. For specific studies (see below), ¹H MAS and ¹³C CP-MAS solid-state NMR spectra were recorded on a Bruker Avance-500 spectrometer with a double-resonance 4 mm CP-MAS probe. The samples were introduced under Ar within a glovebox into a zirconia rotor, which was then tightly closed. In all experiments, the rotation frequency was set to ca. 10 kHz. Chemical shifts were given with respect to TMS as external reference for ¹H and ¹³C NMR.

(46) Mortensen, J. J.; Parrinello, M. *J. Phys. Chem. B* **2000**, *104*, 2901–2907.

(47) Joubert, J.; Delbecq, F.; Thieuleux, C.; Taoufik, M.; Blanc, F.; Coperet, C.; Thivolle-Cazat, J.; Basset, J. M.; Sautet, P. *Organometallics* **2007**, *26*, 3329–3335.

(48) Cheon, J.; Dubois, L. H.; Girolami, G. S. *J. Am. Chem. Soc.* **1997**, *119*, 6814–6820.

Heteronuclear Correlation Spectroscopy. The two-dimensional heteronuclear correlation experiments were performed according to the following scheme: 90° proton pulse, t_1 evolution period, cross-polarization (CP) to carbon spins, detection of carbon magnetization under TPPM decoupling.⁴⁹ The contact time for CP was set to 1 ms. A total of 64 t_1 increments with 1024 scans each was collected, and the recycle delay was 1 s (total acquisition time of 18 h).

J-Resolved Spectroscopy. The two-dimensional J -resolved experiment was performed as previously described:^{28,31} after cross-polarization from protons, carbon magnetization evolves during t_1 under proton homonuclear decoupling. Simultaneous 180° carbon and proton pulses are applied in the middle of t_1 to refocus the carbon chemical shift evolution while retaining the modulation by the heteronuclear J_{CH} scalar couplings. A Z-filter is finally applied to allow phase-sensitive detection in ω_1 . The proton rf field strength was set to 83 kHz during t_1 (FSLG decoupling^{50,51}) and acquisition (TPPM decoupling⁴⁹). The lengths of carbon and proton 180° pulses were 7 and 6 μ s, respectively, and the Z-filter delay was 200 μ s. An experimental scaling factor, measured as already described, of 0.52 was found; this gave a corrected spectral width of 2452 Hz in the ω_1 dimension.⁵² The recycle delay was 2 s, and a total of 80 t_1 increments with 1024 scans each was collected (total acquisition time 30 h).

Two-Dimensional Double-Quantum (DQ) Experiments. These were performed according to the following scheme: excitation of DQ coherences, t_1 evolution, reconversion into observable magnetization, Z-filter, and detection. Fourteen pC7 basic elements⁵³ were used for both excitation and reconversion steps, with 70 kHz rf field strength ($=7\omega_R$); the Z-filter delay was 200 μ s. A total of 512 increments of 64 scans each was collected with 1.5 s recycle delay, which gave a total experiment time of 14 h.

ESR Characterizations. For these measurements, a sample was loaded in a 4 mm quartz tube in a glovebox and then sealed under vacuum. ESR spectra were recorded at room temperature and at 77 K on a Varian E9 spectrometer at ENS-Lyon (Ecole Normale Supérieure, Lyon) and compared to a vanadyl sulfate standard recorded under the same conditions. After a double integration of both signals, the amount of Ti^{III} species could be estimated.

Preparation of Tetrakis(2,2-dimethylpropyl)titanium(IV) (1). The molecular precursor [Ti(CH₂tBu)₄] (1) was prepared from [Ti(OEt)₄] and *t*BuCH₂Li, following the literature procedure (yield 62%).⁴⁸

Preparation of ¹³C-Labeled Tetrakis(2,2-dimethylpropyl)titanium(IV) (1*). The preparation of 1* was performed according to the same procedure as that used for 1, but starting with a 70:30 mixture of nonlabeled *t*BuCH₂Cl and 99% ¹³C-monolabeled *t*Bu*CH₂Cl to form 30% ¹³C-labeled *t*Bu*CH₂Li as alkylating agent (yield 60%).

Preparation of SiO₂-Al₂O₃₋₍₅₀₀₎. Silica-alumina HA-S-HPV from Akzo-Nobel, with 25% of aluminum and a specific area of 478 m²/g, was calcined at 500 °C under dry air flow for 4 h and partly dehydroxylated at 500 °C under high vacuum (10⁻⁵ Torr) for 24 h to give a white solid having a specific surface area of 390 m²/g and containing 1.4 OH/nm² (0.91 mmol/g).

Preparation of 2 by impregnation of 1 onto SiO₂-Al₂O₃₋₍₅₀₀₎. A mixture of 1 [Ti(CH₂tBu)₄] (350 mg, 1.05 mmol) in pentane

(5 mL) and SiO₂-Al₂O₃₋₍₅₀₀₎ (1 g) was stirred at 25 °C for 4 h. After filtration, the solid was washed five times with pentane and all volatile compounds were condensed into another reactor (of known volume) in order to quantify neopentane evolved during grafting. The resulting yellow-brown powder was dried under vacuum (10⁻⁵ Torr) to yield 1.137 g of 2a,b. Analysis by gas chromatography indicated the formation of neopentane during the grafting (1.6 ± 0.2 NpH/Ti). Anal. Found for 2 (wt %): Ti, 2.4–2.9; C, 7.5–8.7. ¹H MAS solid-state NMR (300 MHz): δ 2.4, 1.2 ppm. ¹³C CP/MAS solid state NMR: δ 113, 36, 32 ppm.

Preparation of 2*, by Impregnation of 1* onto SiO₂-Al₂O₃₋₍₅₀₀₎. The ¹³C-enriched surface compounds 2a*,b* were prepared using the procedure described above for the preparation of 2, using 1* in place of 1 with a reaction time of 4 h at 25 °C. Anal. Found for 1* (wt %): Ti, 2.9; C, 8.7. ¹H MAS solid-state NMR (300 MHz): δ 2.4, 1.2 ppm. ¹³C CP/MAS solid state NMR: δ 113, 36, 32 ppm.

Monitoring the Synthesis of [Ti(CH₂tBu)₄]/SiO₂-Al₂O₃₋₍₅₀₀₎ by IR Spectroscopy. The oxide (25 mg) was pressed into an 17 mm self-supporting disk, adjusted in the sample holder, and introduced into a glass reactor equipped with CaF₂ windows. The supports were calcined under air and partly dehydroxylated under vacuum at the desired temperature. Complex 1 was then sublimed under vacuum at 50 °C onto the oxide disk, which typically turned yellow. The solid was then heated at 50 °C for 2 h, and the excess of 1 was removed by reverse sublimation at 50–60 °C and condensed into a tube cooled by liquid N₂, which was then sealed off using a blow torch. An IR spectrum was recorded at each step.

Preparation of 3 by Treatment under H₂ of the Supported Perhydrocarbyl Complexes 2a,b. General Procedure. In a 375 mL reactor, 1 g of sample 2 ([Ti(CH₂tBu)₃]_{SA} and [Ti(CH₂tBu)₂]_{SA}) was treated with 70 kPa of H₂. The temperature was increased to 150 °C (1 °C/min) and was maintained at this temperature for 4 h. The solid turned from yellow to brown. The gaseous products were then quantified by GC: methane (9 equiv of CH₄/Ti) and ethane (1.1 equiv of C₂H₆/Ti). ¹H MAS solid-state NMR (500 MHz, 25 °C): δ (ppm) 0.8 (s, CH), 1.8 (s, SiOH), 4.4 (s, SiH and SiH₂), 8.6 (s, TiH, 3b,c), 9.1 (s, TiH₂, 3a) (deconvolution of the signal with Lorentzian functions: see Figure S4 in the Supporting Information); Infrared (cm⁻¹): 1600–1730 (broad, ν (Ti–H) and ν (TiH₂)), 1910 (ν (Al–H)), 2200, 2260 (m, ν (SiH) and ν (SiH₂)), 2700–2900 (w, ν (C–H)).

Hydrogenolysis of Waxes. General Procedure. Mechanical mixtures of titanium hydrides (75 μ mol of Ti) supported on silica-alumina or on silica and wax (400 mg; Aldrich, ASTM D87; mp 70 °C), were charged using a glovebox into a stainless steel cylinder reactor which could be isolated from the atmosphere (see Figure S5 in the Supporting Information). Two other experiments were carried out similarly, one with a mixture of titanium hydride supported on silica, 200 mg of pure SiO₂-Al₂O₃₋₍₅₀₀₎, and 400 mg of wax and the other being a blank experiment, with a mixture of 200 mg of SiO₂-Al₂O₃₋₍₅₀₀₎ and 400 mg of wax. After connection to the gas lines and purge of the tubes, a flow of hydrogen (20 mL/min), controlled by a mass flow controller (Brooks) under 1 bar of pressure, was sent upward into the catalyst bed, which was heated at 180 °C. Hydrocarbon products were stripped from the liquid medium by the hydrogen flow. Light hydrocarbons and hydrogen were analyzed on line by GC (HP 6890 chromatograph equipped with an Al₂O₃/KCl 50 m × 0.32 mm capillary column and an FID detector for hydrocarbons or with a 3 m molecular sieves column and a catharometer for hydrogen). Liquid products were condensed at 0 °C and analyzed off-line by GC (HP 5890 chromatograph equipped with an HP5 30 m × 0.32 mm capillary column and an FID detector).

(49) Bennett, A. E.; Rienstra, C. M.; Auger, M.; Lakshmi, K. V.; Griffin, R. G. *J. Chem. Phys.* **1995**, *103*, 6951–6958.

(50) Bielecki, A.; Kolbert, A. C.; Levitt, M. H. *Chem. Phys. Lett.* **1989**, *155*, 341–346.

(51) Levitt, M. H.; Kolbert, A. C.; Bielecki, A.; Ruben, D. J. *Solid State Nucl. Magn. Reson.* **1993**, *2*, 151–163.

(52) Lesage, A.; Duma, L.; Sakellariou, D.; Emsley, L. *J. Am. Chem. Soc.* **2001**, *123*, 5747–5752.

(53) Hohwy, M.; Jakobsen, H. J.; Eden, M.; Levitt, M. H.; Nielsen, N. C. *J. Chem. Phys.* **1998**, *108*, 2686–2694.

Acknowledgment. We thank Dr Frédéric Lefèbvre and Sudhakar Chakka for fruitful discussion and the BP Company for financial support.

Supporting Information Available: Figures giving an ^1H MAS NMR spectrum of **2a,b** on silica–alumina₅₀₀, IR spectra on the H/D exchange reaction for the $\text{SiO}_2\text{--Al}_2\text{O}_{3-(500)}$ sup-

ported titanium hydride, an ESR spectrum of the solid **3** Ti species supported on silica–alumina₅₀₀, deconvolution with Lorentzian functions of the ^1H MAS NMR signal of the titanium hydrides **3**, supported on silica–alumina₅₀₀, and a scheme of the reactor used for the wax hydrogenolysis. This material is available free of charge via the Internet at <http://pubs.acs.org>.